Supporting Information

Comparison of Two Yeast MnSODs: Mitochondrial *Saccharomyces cerevisiae* versus Cytosolic *Candida albicans*

Yuewei Sheng,[†] Troy A. Stich, [§] Kevin Barnese,[†] Edith B. Gralla,[†] Duilio Cascio,[‡] R. David Britt, [§] Diane E. Cabelli, [*,∥] Joan Selverstone Valentine[*,†,⊥]

[†]Department of Chemical and Biochemistry, and [‡]Department of Energy-Institute for Genomics and Proteomics, University of California Los Angeles, 420 Westwood Plaza, Los Angeles, California 90095, United States

[§]Department of Chemistry, University of California Davis, One Shields Avenue, Davis, California 95616, United States

[||]Chemistry Department, Brookhaven National Laboratory, Upton, New York 11973, United States

[⊥]Department of Bioinspired Scienses, Ewha Womans University, Seoul 120-750, Republic of Korea

Table of Contents:

Complete Reference for Ref. 37

Figure S1: ESI-MS of methylated *Sc*MnSOD

Figure S2: SDS-PAGE gel of purified *Ca*MnSODc

Figure S3: *Ca*Mn^{3+}SODc trace generated in pulse radiolysis

Figure S4: Comparison of kinetics of *Ca*MnSODc and *Sc*CuZnSOD

Figure S5: Product inhibition of *Ca*MnSODc at different pH

Figure S6: Oxidation state of *Ca*MnSODc

Figure S7: The deconvolution of the 390 nm absorption intensity

Figure S8: Optical spectra of anion-bound *Sc*MnSOD

Figure S9: Oxidation of *Sc*MnSOD by O_2^- at long time scales

Figure S10: The Mn^{3+} spectra of yeast MnSODs at different pH as determined by pulse radiolysis

Figure S11: EPR spectra of as-isolated *Sc*MnSOD and *Ca*MnSODc

Figure S12: Temperature dependence of parallel-mode EPR spectra

Figure S13: The quaternary structure of *Sc*MnSOD and *Ca*MnSODc

Figure S14. Superposition of the active site of *Sc*MnSOD and *Ca*MnSODc

Table S1: X-ray data collection and refinement statistics

Table S2: Active site crystallographic distances of yeast, human and bacterial MnSODs

Ref. 58: Wang, W.; Fang, H.; Groom, L.; Cheng, A.; Zhang, W.; Liu, J.; Wang, X.; Li, K.; Han, P.; Zheng, M.; Yin, J.; Mattson, M. P.; Kao, J. P.; Lakatta, E. G.; Sheu, S. S.; Ouyang, K.; Chen, J.; Dirksen, R. T.; Cheng, H. *Cell* **2008**, *134*, 279.

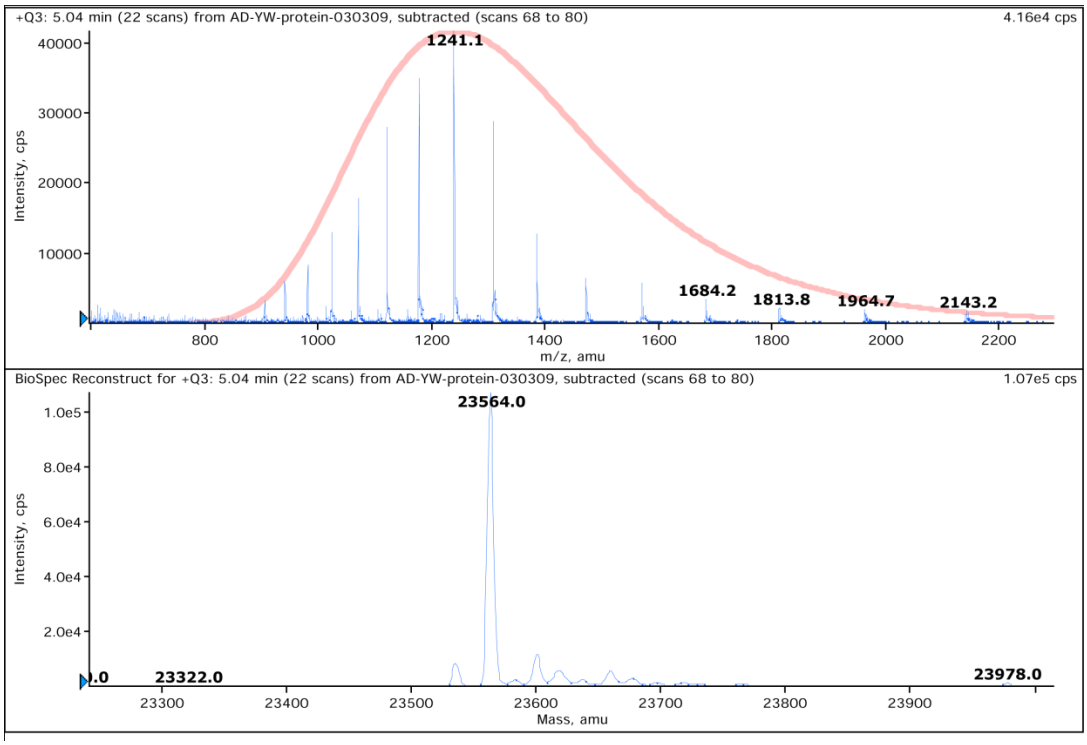

Figure S1. Electrospray-ionization mass spectra (top panel) of methylated *Sc*MnSOD and its reconstructed mass distribution profiles (bottom panel). Ordinate units of intensity are arbitrary and the abscissa units of average molecular mass are in Daltons. The expected mass is 23,560 Da.

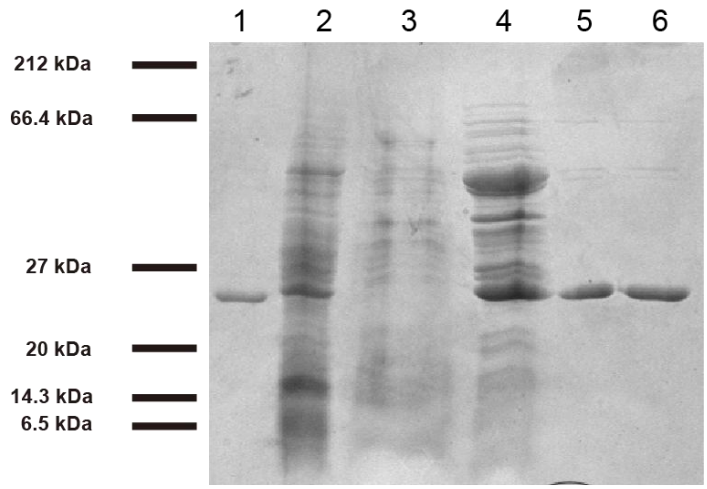

Figure S2. The SDS-PAGE analysis of the purification of *Ca*MnSODc: 1) purified *Sc*MnSOD; 2) cell lysate; 3) supernatant of ammonium sulfate cut; 4) active HIC fractions; 5) DE52 load and wash; 6) 5 μg of purified *Ca*MnSODc after G300 column.

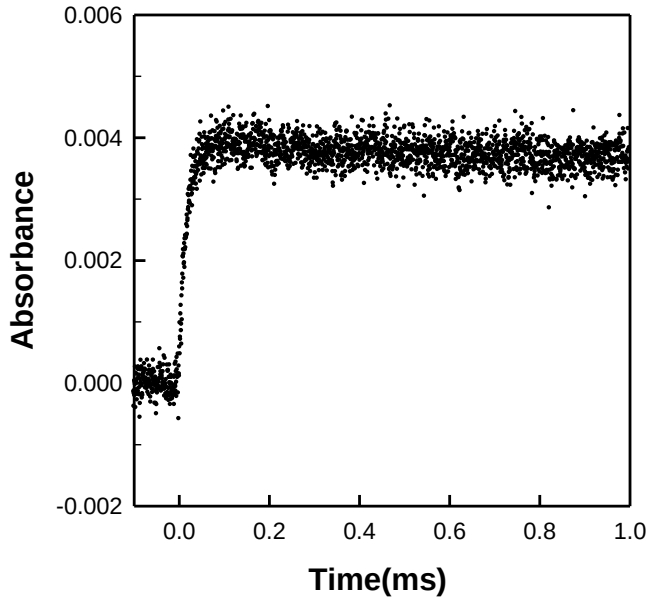

Figure S3. The oxidation of *Ca*Mn^{2+}SODc by O_2^- in pulse radiolysis. The formation of Mn^{3+}SOD is indicated by the change of absorbance at 480 nm over time upon generation of 2.2 μM O_2^-. The sample contained 60 μM (in Mn) *Ca*MnSODc, 10 mM potassium phosphate (pH 7), 10 mM sodium formate, and 100 μM EDTA. The enzyme was reduced prior to each pulse with 120 μM H_2O_2.

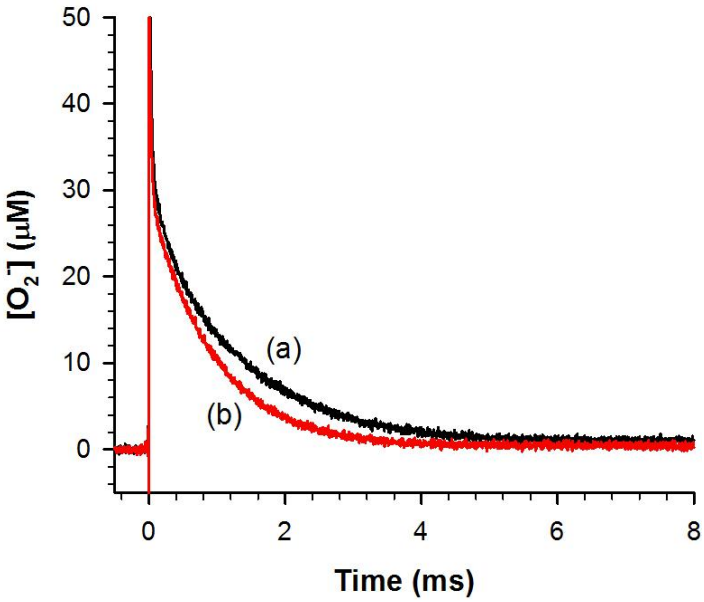

Figure S4. Decay of 48 μM O_2^- catalyzed by 1 μM (in Mn) *Ca*MnSODc (a, black) and *Sc*CuZnSOD (b, red). The sample of pulse radiolysis contained 10 mM potassium phosphate (pH 7), 10 mM sodium formate and 10 μM EDTA.

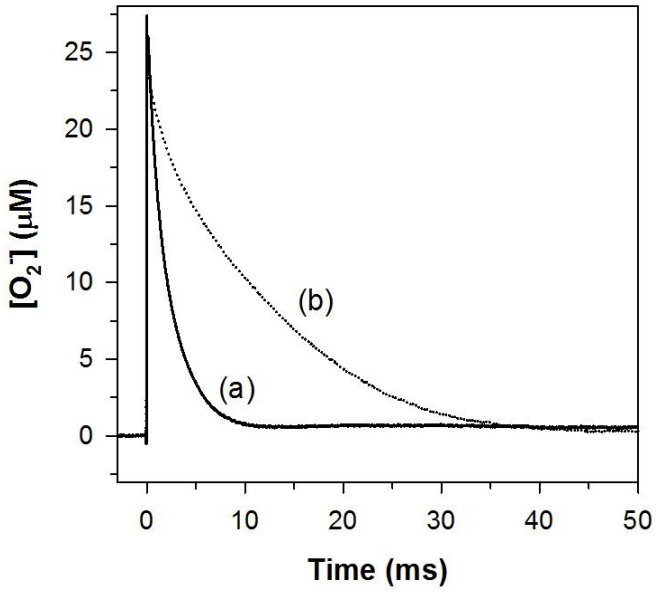

Figure S5. Dependence of the level of product inhibition of *Ca*MnSODc on pH. Decay of 25 μM O_2^- catalyzed by 1 μM (in Mn) *Ca*MnSODc at pH 7.5 (a) and 9.0 (b). The sample of pulse radiolysis contained 10 mM potassium phosphate (pH 7), 10 mM sodium formate and 10 μM EDTA.

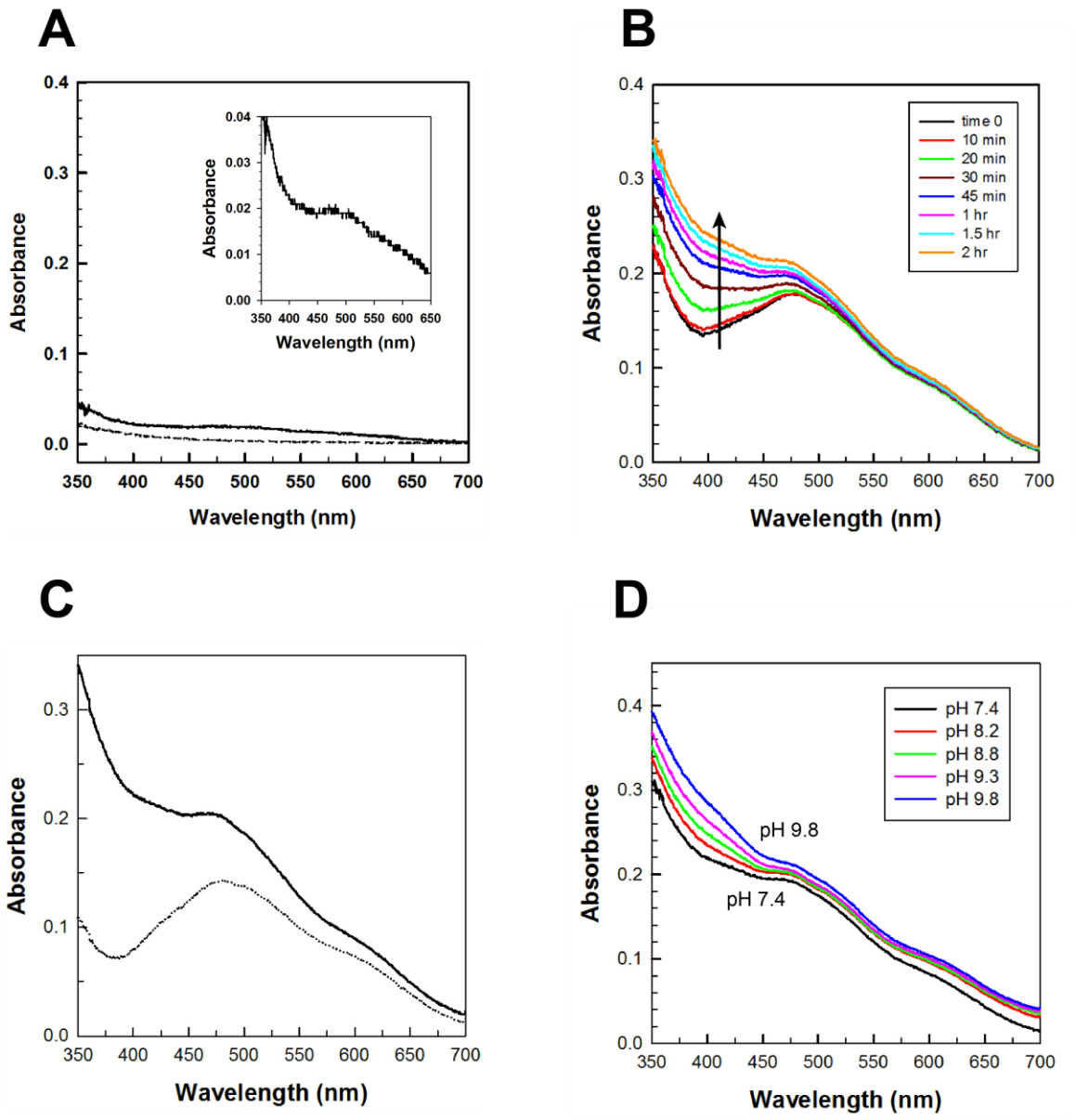

Figure S6. The oxidation state of *Ca*MnSODc. (**A**) Optical spectra of as-isolated *Ca*MnSODc (solid line) and *Ca*MnSODc reduced by sodium hydrosulfite (dashed line). Inset: The difference spectrum between as-isolated and reduced *Ca*MnSODc. (**B**) Optical spectra of *Ca*MnSODc oxidized by potassium permanganate ([$KMnO_4$]:MnSOD = 0.75:1) as measured over time. (**C**) Reduction of *Ca*Mn^{3+}SODc (solid line, oxidized by 0.75 equivalent of $KMnO_4$ and allowed to equilibrate at room temperature for 2 hr) by one equivalent of sodium ascorbate (dotted line). (**D**) Optical spectra of *Ca*Mn^{3+}SODc at different pH. The sample solution contained 160 μM (in Mn) enzyme in 25 mM potassium phosphate (pH 7.4).

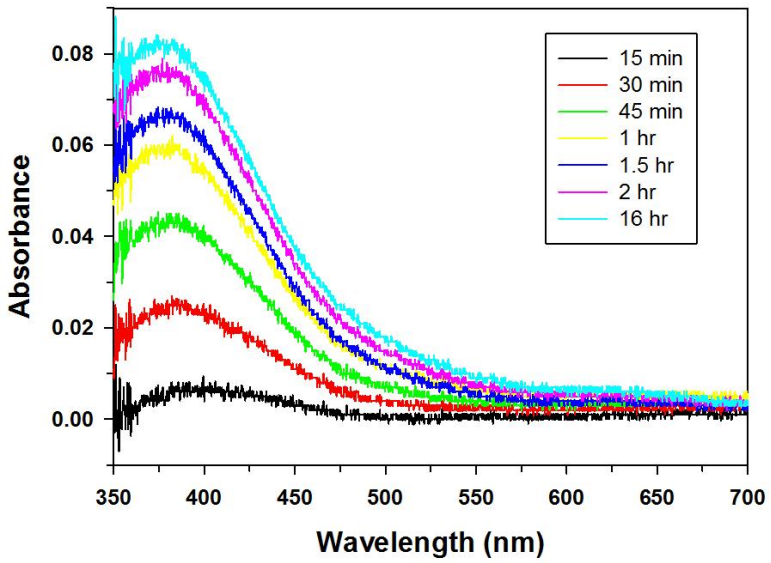

Figure S7. The deconvoluted absorption band of *Sc*Mn^{3+}SOD around 390nm as measured over time. *Sc*MnSOD was oxidized by potassium permanganate ([$KMnO_4$]:MnSOD = 0.75:1) at pH 7.4. Time 0 refers to the start of the first scan immediately after mixing $KMnO_4$ with the enzyme.

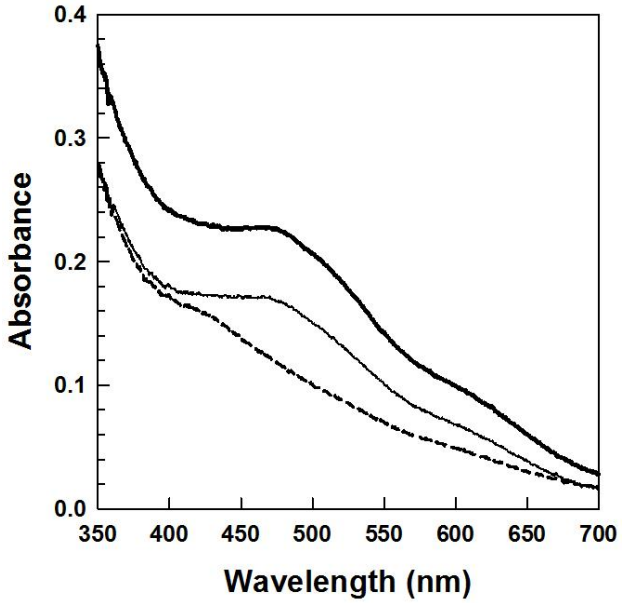

Figure S8. Anion binding causes spectral shifts of *Sc*Mn^{3+}SOD. Solutions contained 190 μM (in Mn) *Sc*MnSOD oxidized by 0.75 equivalent of $KMnO_4$ (thick solid, allowed to equilibrate at room temperature for 2 hr) in 25 mM potassium phosphate (pH 7.4) with 100 mM NaF (thin solid) and 100 mM NaN_3 (dashed).

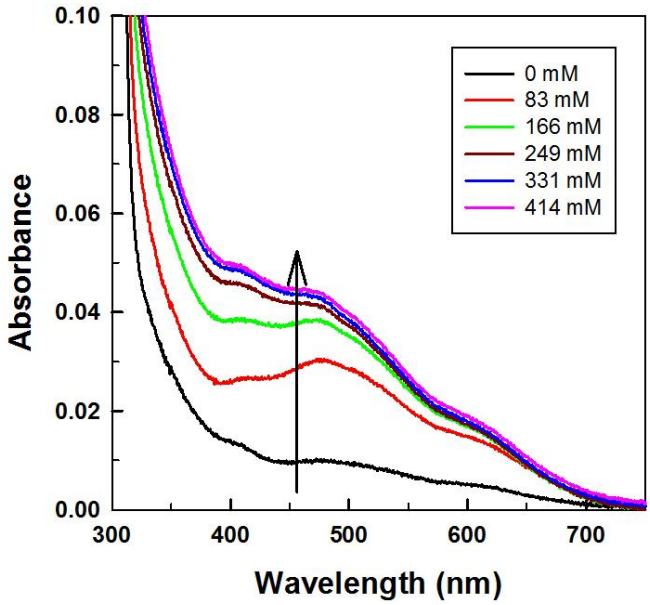

Figure S9. Oxidation of as-isolated *Sc*MnSOD by O_2^- at long timescales. O_2^- was generated by ^{60}Co radiation source. The legend shows the doses of O_2^- that reacted with *Sc*MnSOD before spectra were taken. The sample solution contained 130 μM (in Mn) *Sc*MnSOD in 25 mM potassium phosphate (pH 7.4) and 200 units/mL catalase.

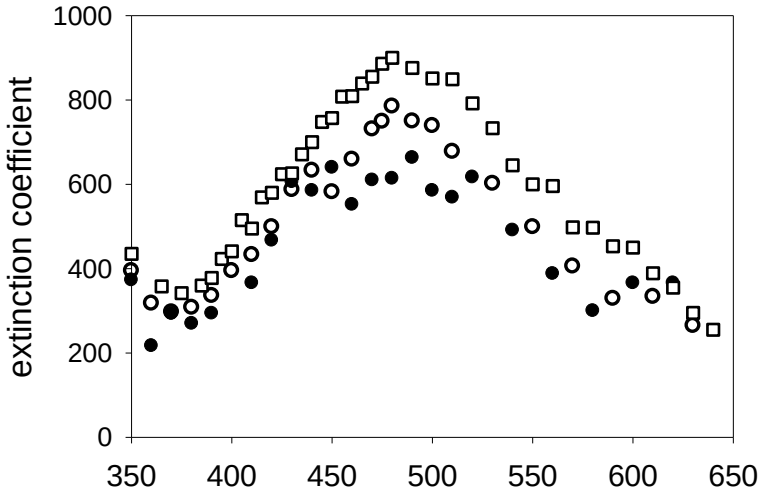

Figure S10. The Mn^{3+} spectra of yeast MnSODs at different pH as determined by pulse radiolysis. Protein samples are: 1) 60 μM *Ca*MnSODc at pH 7.5 (squares); 2) 40 μM *Sc*MnSOD at pH 7.0 (open circles); 3) 40 μM *Sc*MnSOD at pH 10.0 (closed circles).

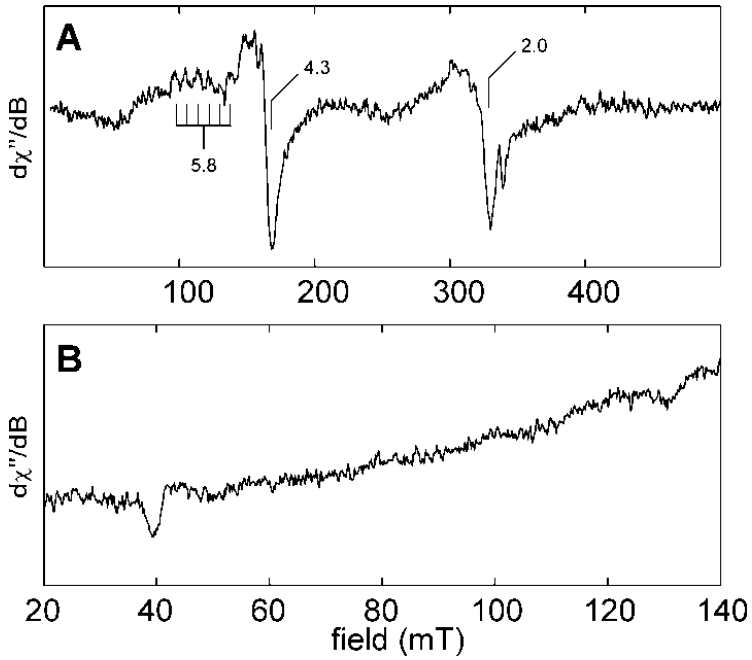

Figure S11. These spectra are similar to those obtained for *Ec*Mn^{2+}SOD. Five separate electron spin transitions are possible and these are shifted from $g = 2.0$ due to zero-field splitting of the manifold of spin levels of the high-spin ($S = 5/2$) Mn^{2+} ion. In some cases, these resonances are further split (e.g., the feature at $g = 5.8$) by the hyperfine interaction of the electron spin with the ^{55}Mn nuclear spin ($I = 5/2$).

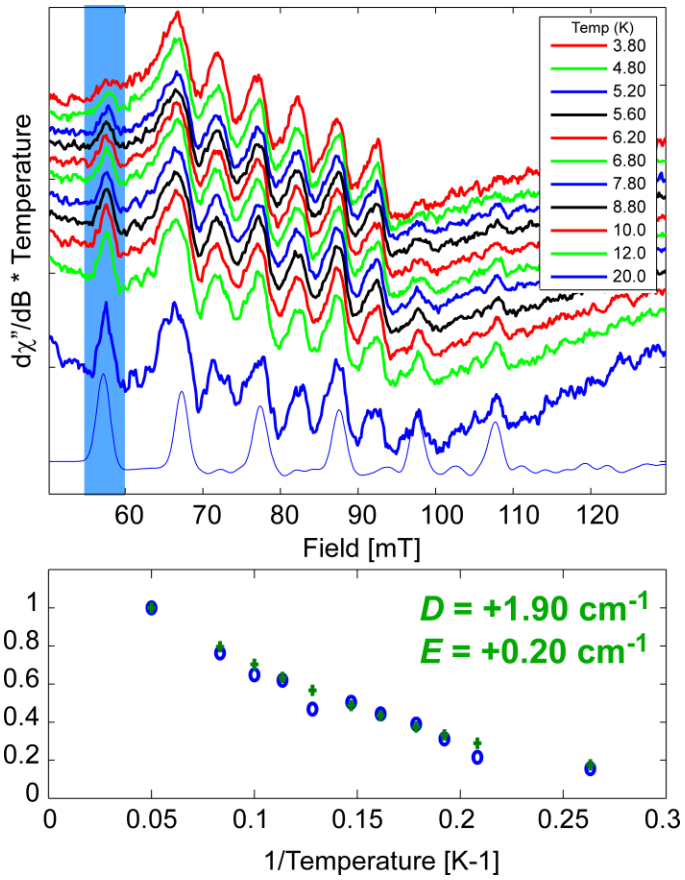

Figure S12. (Top panel) Temperature dependence of the parallel-mode EPR spectrum of permanganate-oxidized *Ca*MnSODc. Except for temperature (given in legend), the spectrometer settings are the same as those given in the caption of Figure 7. Simulation of the $^5A_{1g}$ component is shown (thin blue line). (Bottom panel) Integrated intensity of feature centered at 58 mT (blue circles) as a function of the inverse of the temperature and corresponding simulated integrated intensity (green crosses) achieved using ZFS parameters D = +1.90 cm^{-1} and E = 0.2 cm^{-1}.

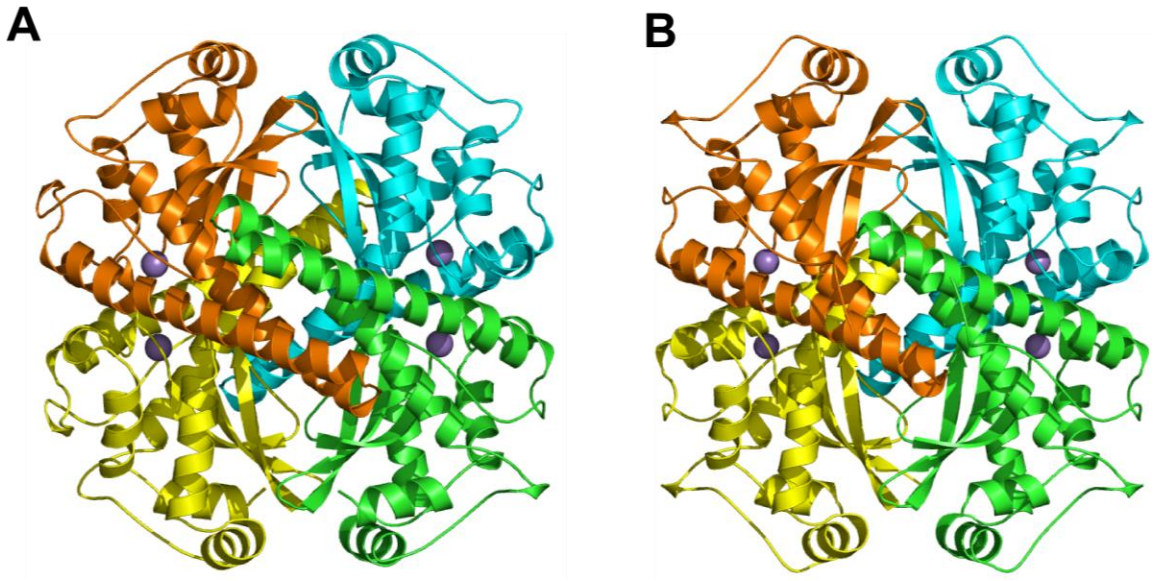

Figure S13. The quaternary structure of *Sc*MnSOD (**A**) and *Ca*MnSODc (**B**) in crystal lattice. Crystallization condition for *Ca*MnSODc: 0.1 M magnesium chloride, 0.1 M sodium chloride and 0.1 M tri-sodium citrate (pH 5.5) in 30% (w/v) polyethylene glycol 400 at 4 °C with a protein concentration of 7 mg/mL.

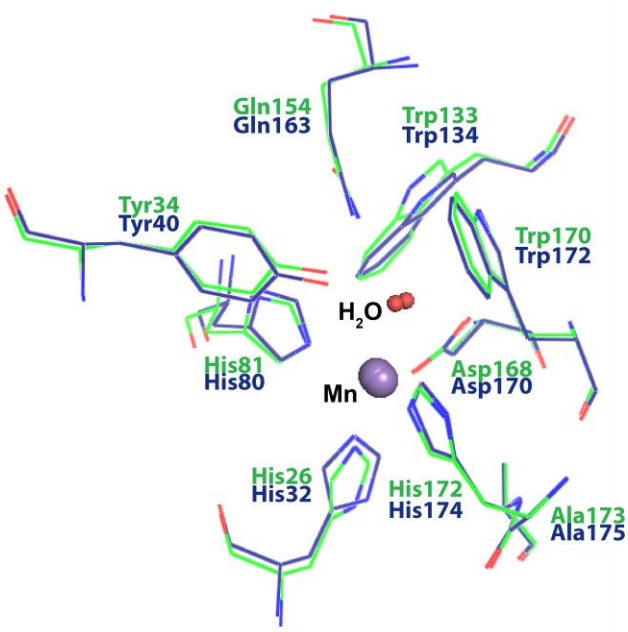

Figure S14. Superposition of the active site of *Sc*MnSOD (green, chain A, PDB accession: 3LSU) and *Ca*MnSODc (blue, PDB accession: 3QVN).

Table S1. X-ray Data Collection and Refinement Statistics [a].

	***Sc*MnSOD**	***Ca*MnSODc**
Data Collection		
X-Ray Source	Rigaku FRE+	Rigaku FRE+
Detector	Rigaku HTC	Rigaku HTC
Reflections observed	197227	252317
Unique reflections	59997	6933
Wavelength (Å)	1.5418	1.5418
Resolution (Å)	1.90	2.60
Highest Resolution Shell (Å)	1.97-1.90	2.69-2.60
Space group	P1	P $6_4$22
R_{sym} (%) [b]	8.3 (31.4)	17.9 (74.3)
I/σ	14.8 (3.7)	22.9 (8.1)
Completeness (%)	89.5 (53.1)	99.0 (100.0)
Unit cell dimensions		
a (Å)	63.657	77.134
b (Å)	64.933	77.134
c (Å)	66.550	120.080
α (°)	109.36	90.0
β (°)	106.33	90.0
γ (°)	109.68	120.0
Wilson B value ($Å^2$)	24.3	52.8
Refinement		
Resolution (Å)	32.0 – 1.9	44.6 – 2.6
Reflections Used	59979	6626
R_{work}(%)	16.30 (16.50)	20.25 (27.42)
R_{free} (%) [c]	19.50 (19.20)	26.86 (40.48)
Protein Molecules in Asymmetric Unit	4	1
Number of non-H atoms		
Protein	6661	1593
Non-protein	450	23
RMS deviations		
Bond lengths (Å)	0.007	0.002
Bond angles (°)	1.045	0.517
Average B-factor ($Å^2$)		
Protein atoms	24.52	52.85
Non-protein atoms	29.50	40.75
PDB accession code	3LSU	3QVN

a. Highest resolution shell shown in parenthesis.
b. $R_{sym} = \Sigma | I-<I> | / \Sigma I$
c. R_{free} calculated using 5% of the data

Table S2. Active Site Crystallographic Distances

	*Sc*MnSOD (pdb: 3lsu)	*Ca*MnSODc (pdb: 3qvn)	Human (pdb: 1n0j)	*A. fumigatus* (pdb: 1kkc)	*C. elegans* (pdb: 3dc5)	*E. coli* (pdb: 1vew)	*T. Thermophilus* (pdb: 3mds)	*Drad* (pdb: 2ce4)
Ligands								
Mn-NE2 (His26)[a]	2.24 (0.05)	2.35	2.10 (0.01)	2.11 (0.09)	2.23 (0.01)	2.14 (0.04)	2.14 (0)	2.19 (0.05)
Mn-NE2 (His81)	2.22 (0.02)	2.27	2.10 (0.02)	2.19 (0.06)	2.19 (0.01)	2.21 (0.01)	2.10 (0.02)	2.10 (0.09)
Mn-NE2 (His172)	2.22 (0.02)	2.26	2.09 (0)	2.20 (0.08)	2.18 (0.07)	2.17 (0.01)	2.17 (0.02)	2.16 (0.08)
Mn-OD2 (Asp168)	2.05 (0.02)	2.11	1.94 (0)	1.99 (0.04)	2.06 (0.01)	2.02 (0.01)	1.79 (0.01)	1.93 (0.04)
Mn-O (coord solvent)	2.31 (0.04)	2.33	2.02 (0.01)	2.27 (0.06)	2.26 (0.01)	2.21 (0.05)	2.08 (0.01)	2.19 (0.01)
Coordinating Solvent Molecule								
O-OD2 (Asp168)	2.89 (0.03)	3.08	2.95 (0.06)	2.89 (0.11)	2.78 (0)	2.78 (0.04)	2.78 (0.06)	2.83 (0.01)
O-ND (Gln154)	2.95 (0.02)	2.92	2.95 (0.01)	2.78 (0.13)	2.86 (0.01)	2.90 (0.08)	2.99 (0.03)	2.87 (0.06)

a. Numbering in *Sc*MnSOD is use